Cellular and Molecular Biology™ **47** (7), 1229-1239
Printed in France.

0145-5680/01
2001 Cell. mol. Biol.™

IDENTIFICATION OF GENES EXPRESSED IN THE *XENOPUS* INNER EAR

Elba E. SERRANO✉, Casilda TRUJILLO-PROVENCIO, David R. SULTEMEIER, W. Michael BULLOCK and Quincy A. QUICK

Department of Biology, Box 30001-3AF, New Mexico State University, Las Cruces, New Mexico 88003, USA
Fax: +1 505 646 5665; E-mail: eserrano@nmsu.edu

Received February 26, 2001; Accepted July 19, 2001

Abstract - Recent studies indicate that hearing loss in humans has strong hereditary components associated with expression of specific genes in the auditory apparatus of the inner ear. However, the inner ear poses challenges for molecular research because the amount of tissue that can be isolated is limited, and extraction procedures yield small quantities of RNA and protein. To begin to identify genes essential for auditory function, we synthesized a cDNA library using an RT-PCR protocol and total RNA isolated from eight *Xenopus laevis* inner ears. Sequence analysis of randomly selected clones demonstrated expression of both identified (calmodulin, SNARE protein, syndecan-2) and unidentified genes, and confirmed synthesis of full length transcripts. Confocal and scanning electron microscopy (SEM) were used to examine the structure of inner ear organs that serve as auditory receptors in amphibians: the sacculus, the amphibian papilla and the basilar papilla. SEM images illustrate the heterogeneity of bundle morphology and demonstrate the continuous appearance of stereociliary bundles in the *X. laevis* amphibian papilla during larval development and adult life. Investigations of gene expression in *Xenopus* auditory organs using clones recovered from inner ear cDNA libaries should provide insight regarding the molecular basis of hearing.

Key words: *Xenopus*, inner ear, auditory, vestibular, hair cell, confocal, SEM, stereocilia, amphibian papilla, sacculus, basilar papilla, cDNA library, SMART cDNA synthesis, development

INTRODUCTION

Hearing loss is believed to be the most prevalent sensory disorder in humans (39). In the U.S., almost 30 million Americans are deaf or hearing impaired, and millions more are exposed to potentially harmful environmental factors such as damaging levels of noise (22). By the age of 65, over 25% of people experience hearing impairment, while by the age of 80, almost 50% are affected (8). Hereditary deafness affects 1 in 2000 children (37), and in the U.S. over 800,000 children between 6-19 years of age have some hearing impairment (28). Furthermore, recent reports raise concerns that health disparities that are correlated with differences in race/ethnicity may exist in the general population. For example, the age of diagnosis of sensorineural hearing impairment in Caucasian children is much earlier than in Black or Hispanic children, independent of socioeconomic status (26). There also is evidence that differences exist in the prevalence of bilateral childhood hearing loss between African-American, Cuban-American, Mexican-American, Puerto Ricans and non-Hispanic white children (28).

Over half of sensorineural hearing loss is believed to have a genetic component (42). Mutations in over thirty genes including connexin-26, myosin VIIa, α-tectorin, and POU4F3 have been shown to give rise to hearing disorders (8,21,22,39). In recent years, progress has been made toward determining how mutations in some of these genes can lead to hearing loss. For example, myosin VIIA

Abbreviations: **AP**: amphibian papilla; **BP**: basilar papilla; **CLSM**: confocal laser scanning microscope; **cz**: central zone; im: inner margin; **LD-PCR**: long distance polymerase chain reaction; om: outer margin; **PBS**: phosphate buffered saline; **RT-PCR**: reverse transcriptase polymerase chain reaction; **SAC**: sacculus; **SEM**: scanning electron microscopy; **0**: switch mechanism at the 5' end of RNA templates

is an unconventional myosin that is expressed in hair cells of the cochlea. Evidence suggests that this protein may play a role in membrane turnover at the apical hair cell surface (35), cell-cell adhesion (27) and stabilization of stereociliary bundle structure (18,27). Disruption of these functions could incapacitate hair cells and contribute to hearing loss. In contrast, mutations in connexin-26, a gap junction protein expressed in the inner ear, are believed to cause hearing loss by disrupting normal potassium recycling and osmotic balance in the cochlea (29,36).

These findings have prompted efforts to identify additional genes responsible for hereditary deafness with the goal of developing treatments and therapies for hearing loss. In addition, since a prominent cause of hearing impairment is loss or damage to the mechanosensory hair cells of the inner ear, there is specific interest in identifying genes expressed in these cell types (8,22). Research advances in this area rely on the use of animal models such as chick, mouse, amphibians, and reptiles (8,13,45), along with the development of molecular approaches that are compatible with the small amount of tissue and overall inaccessibility of the auditory organs of the inner ear (19,34).

We seek to identify genes expressed in the inner ear, and are using the amphibian *Xenopus laevis,* to this end. *X. laevis* has long been an effective heterologous expression system, and a model organism for cellular and developmental studies (25). In recent years, several laboratories have realized the potential of *X. laevis* as a useful system for investigations of auditory and vestibular development during inner ear organogenesis and morphogenesis (5,9,15,16,33). In amphibians like *X. laevis*, the inner ear contains eight sensory endorgans specialized to respond to different stimuli and various frequencies (10, 30, 31). Each endorgan contains a sensory epithelium comprised of mechanosensory hair cells that are innervated by branches of the eighth cranial nerve (51). Anatomical and physiological studies in anurans have shown that the amphibian papilla (AP) and the basilar papilla (BP) are specialized for reception of acoustical signals of different frequencies (10,30,31). The sacculus (SAC) responds to both acoustic and seismic stimuli (30,31). The auditory sensitivity of the *X. laevis* inner ear lies between 200-3900 Hz, a range comparable to that of similarly sized terrestrial anurans (11). The BP is responsive to high (>1000 Hz) frequencies, the AP to intermediate (100-1400 Hz) frequencies and the SAC to low (<300 Hz) frequencies (30,31,51). In some amphibians, a transient period of "deafness" can be observed during metamorphosis (4).

Studies of amphibians have provided fundamental understanding of mechanosensory transduction by hair cells (23,44). Of particular importance are the findings that amphibians can regenerate (3) and perpetually produce (7,9) mechanosensory hair cells. Therefore, studies of the amphibian inner ear may permit identification of regenerative processes that are virtually absent in humans.

To begin the process of inner ear gene identification, we used the Clontech SMART™ cDNA synthesis protocol to construct a cDNA library from total RNA isolated from eight *Xenopus* inner ears. The SMART™ protocol is designed to enrich for full length clones and to produce representational libraries from small amounts of starting material (20). Both identified and unidentified genes were recovered from the cDNA library, and many clones contained full length sequences. We simultaneously gathered anatomical data from the SAC, AP and BP using confocal microscopy and SEM. In previous studies, we examined the distribution and number of hair cell types throughout development of the *X. laevis* SAC (9), as well as developmental differences in axon growth between the saccular, amphibian papillar, and basilar papillar nerves (33). For this study, we used SEM to examine the development of the AP during larval and post-metamorphic periods of *X. laevis* life, thereby extending previous findings from ultrastructural studies of the anuran inner ear (7,9,32,40,41). Our results provide comparative structural information about the sensory epithelia of the *X. laevis* auditory papillae, as well as an anatomical context for future studies that will examine the expression patterns of genes isolated from the cDNA library.

MATERIALS AND METHODS

Animals

Xenopus laevis (NASCO, Fort Atkinson, WI) used in this study represented a 2 year period of animal life. Larval animals (stage 52, stage 60) were staged according to Nieukoop and Faber (38) and euthanized in 0.25% 3-aminobenzoic acid ethyl ester methanesulfonate salt (Sigma, St. Louis, MO) for 15 min at 4°C. Postmetamorphic animals classified as juveniles (1-2 wk post-metamorphosis), adolescents (3-6 months) and adults (2 years) were euthanized in a 4°C solution of 0.25% 3-aminobenzoic acid ethyl ester methanesulfonate salt for 30 min and then decapitated prior to aseptic surgical removal of inner ear tissue. Inner ears were processed for microscopy or RNA extraction as described below. All procedures were approved by NMSU IACUC.

Confocal laser scanning microscopy

Microdissected auditory and vestibular organs from juvenile *X. laevis* (1-2 wks post metamorphosis) were fixed in 4% formaldehyde for 2 hrs at room temperature. The tissue was decalcified in 0.15 M EDTA at room temperature overnight, then labelled for 2 hr with 6 nM

Alexa 488 (Molecular Probes A-12379) or 12 nM Alexa 568 phalloidin (A-12380) (Molecular Probes, Eugene, OR) to detect the actin cytoskeleton. Microdissected organs were rinsed 3 x 15 min each in PBS, then mounted on SuperFrost Plus slides (MJ Research, Watertown, MA) in slow fade anti-fade reagent (Molecular Probes) in glycerol. A BioRad MRC-1024 confocal laser scanning microscope (CLSM) was used to collect digitized images of the fluorescent-labeled tissue and the BioRad LaserSharp software was used to render confocal sections and projected images of the inner ear from the digitized data.

Scanning electron microscopy

Following decapitation, inner ear organs were dissected and prepared for SEM using an established procedure (9). Some specimens were sonicated for 30 sec prior to post-fixation in 2% osmium tetroxide. Samples were dried by critical-point method with CO_2, then sputter-coated with gold and examined with a Hitachi S-3200N Variable Pressure SEM. Six to ten samples were prepared for SEM at each animal age for each sensory endorgan. The best samples were used for image presentation and data analysis.

RNA extraction

Juvenile *X. laevis* with an average weight of 1.1 ± 0.4 g and an average length of 2.1 ± 0.3 cm were used for RNA extraction. The animals (n= 15) were decapitated prior to aseptic surgical removal of inner ear tissue. After decapitation, the lower jaw was removed and with the aid of a binocular dissecting microscope (Nikon SMZ-2T) the otic capsules were partially opened with a sterile scalpel. A small amount of RNAlater™ (Ambion, Austin, TX), an RNA stabilization solution, was pipetted into the otic capsule and the inner ear tissue was extracted with fine forceps (9). The inner ear tissue was placed in RNAlater™ (Ambion, Austin, TX) and stored overnight at 4°C. Total RNA was isolated using a RNAqueous™-4PCR isolation kit (Ambion, Austin, TX). The kit incorporates a DNase step to ensure that isolated RNA is DNA-free. Total RNA (8.3 μg) was isolated from 30 inner ears (40 mg).

cDNA synthesis and library construction

A portion (2 μg) of the isolated total RNA from inner ear tissue was used as the starting material for cDNA library construction using a SMART™ cDNA Library Construction kit (Clontech, Palo Alto, CA). Parallel RT and PCR control reactions were conducted using RNA supplied by the manufacturer. First strand cDNA was synthesized with Superscript™ II reverse transcriptase (Life Tecnologies, Gaithersburg, MD). One fifth of the first strand cDNA reaction was then amplified by long distance PCR. After size selection, cDNA was ligated to the λTriplEx2™ vector provided in the Clontech kit (two reactions: 133 ng or 200 ng) and then packaged in MaxPlax™ Lambda Packaging Extracts (Epicentre Technologies, Madison, WI). One and a half million primary library clones were amplified.

Actin screen

A *X. laevis* β-actin probe was synthesized by incorporation of digoxigenin (DIG)-11-dUTP (Boehringer Mannheim, Indianapolis, IN) during PCR cycling from a plasmid template. For the actin screen, aliquots of 25,000 plaque forming units from the amplified library were plated on 150 mm agar plates. The plaques were lifted onto nylon membranes, denatured, and the DNA fixed by UV crosslinking. The membranes were used for Southern hybridization according to the DIG System User's Guide for Filter Hybridization (Boehringer Mannheim) using 5 ng/ml of DIG-labelled β-actin probe. After hybridization and post-hybridization washes, the chemiluminescent substrate, CDP-Star™ (Boehringer Mannheim), was used to detect positive signals and the percent actin representation of the cDNA library was then calculated.

Random clone analysis

The amplified library was plated and 50 random clones were excised following the manufacturer's protocol (Clontech, Palo Alto, CA). Plasmid DNA was prepared using a modified alkaline lysis plasmid miniprep procedure (50). Insert sizes were determined by digesting the isolated plasmid DNA with Sfi I restriction endonuclease

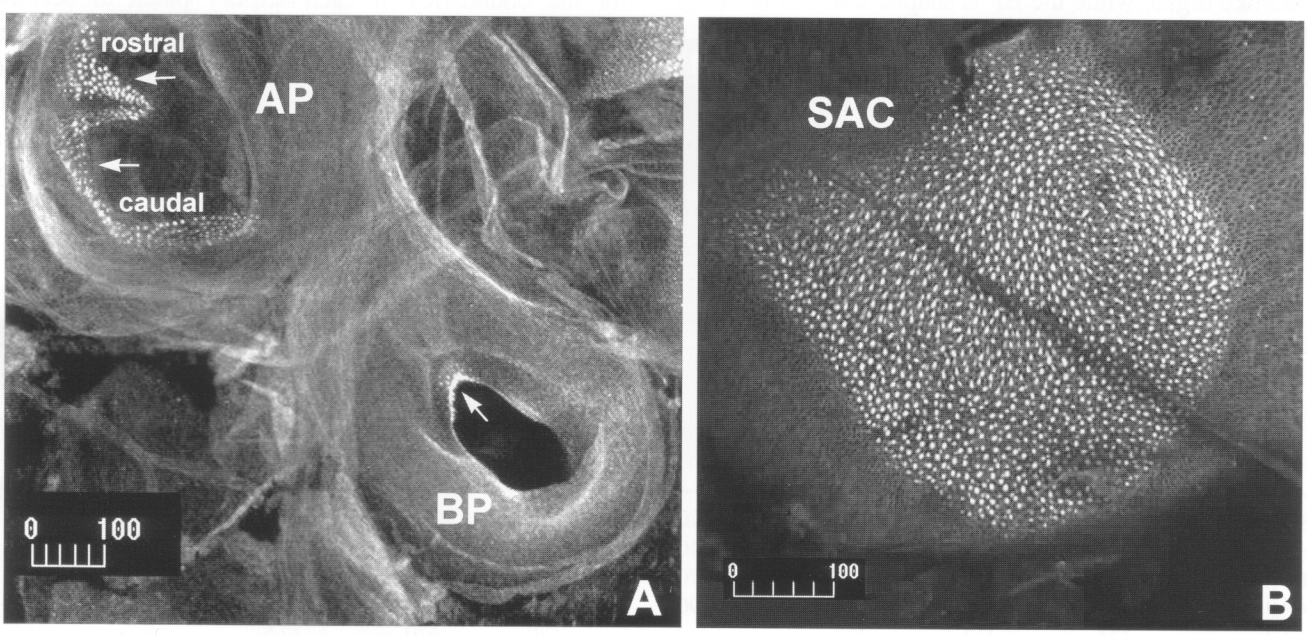

Fig. 1 Confocal projections of three *Xenopus* inner ear organs labelled with Alexa 488 phalloidin. Arrows point to regions containing hair cell bundles that appear as bright punctate spots on the sensory epithelia. **A**) Juvenile *Xenopus laevis* amphibian (AP) and basilar (BP) papilla. **B**) Juvenile *Xenopus laevis* sacculus. Scale bar 100 μm

(New England Biolabs, Beverly, MA), and electrophoreses of restriction digests on a 0.8% agarose gel. Recombinant plasmids that contained insert sizes of 1 kb or above were isolated using a QIAprep Miniprep kit (Qiagen, Valencia, CA). The isolated plasmid DNAs were used as templates for PCR cycle sequencing. Labeled primers (T7 and a λTriplEx2 specific primer) containing a single infrared fluorescent cyanine dye (LI-COR, Lincoln, NE) were used in the cycle sequencing with a SequeTherm™ Excel II sequencing kit (Epicentre Technologies, Madison, WI). Sequencing reaction products were electrophoresed on a 6% Long Ranger™ gel (FMC, Rockland, MA) that was cast in the gel apparatus of the LI-COR 4200 Dual Laser Sequencer System. Data collection and base calls were carried out by the Base ImagIR™ Sequencing Software version 2.2 (LI-COR, Lincoln, NE). Sequences from both strands were analyzed for sequence similarity to GenBank entries using BLAST sequence similarity searching (http://www.ncbi.nlm.nih.gov/blast/blast.cgi?Jform=0).

RESULTS

Confocal imaging of the amphibian papilla (AP), basilar papilla (BP) and sacculus (SAC)

Whole mounts of microdissected auditory organs were readily labelled with fluorescent phalloidin. With CLSM the sensory field could be identified from the patterns formed by the intense fluorescence of the actin-rich stereociliary bundles of the organs (Fig. 1). The bundles appear at low magnification as bright punctate dots distributed in patterns that resemble those visible in SEM images of the AP (Fig. 2A-2E), BP (Fig. 2F) and the SAC (9). The confocal projections of the three sensory organs portrayed here differ in gross morphology. The AP is a pod-like organ, while the BP is shaped like a donut (Fig. 1A). The SAC specimen was prepared with a decalcification step, in order to remove the otoconia that lie over the sensory field. The SAC is the largest and most easily identifiable organ in the *X. laevis* inner ear, resembling a sphere innervated by several thin stalks (33).

The confocal projections illustrate the unique sensory fields of the three endorgans, as well as the variation in the number of stereociliary bundles between the organs. The AP sensory epithelium (Fig.1A, 2A-2E) contains two clearly identifiable areas, a triangular rostral patch, and a horseshoe-shaped caudal patch. The open end of the horseshoe faces the medial wall of the papilla and the curved portion faces the lateral end of the papilla at the papillo-saccular foramen. The BP sensory epithelium is a single heel-shaped patch on the lumen of the organ. The AP and BP sensory patches could be divided into a central zone (cz), an outer margin (om) and an inner margin (im). The sensory field of the SAC contains a central zone with a hoof-print shape and a peripheral zone at the edge of the sensory field. The confocal image shown here is comparable to those previously reported with SEM (9). When organs from the same age are compared, it is apparent that the SAC contains the most stereociliary bundles, the AP has a lesser amount, while the BP contains the least number of stereociliary bundles of the three auditory organs.

SEM of the amphibian papilla

The AP epithelium is intimately joined to the overlying tectorial mass. Due to this configuration, preparation of clean SEM specimens is technically challenging, particularly in the older specimens. The sensory epithelium is similarly shaped at all ages, with a tendency for the boundaries of each sensory patch to become progressively less distinct but still discernable in older animals (Fig. 2). The sensory field increases in length and area from larval (Fig. 2A, 2B, Table 1) through post-metamorphic life (Fig. 2C-2E, Table 1), with a corresponding increase in the number of stereociliary

Table 1 Number of hair cell stereociliary bundles and sensory patch dimensions of the amphibian papilla during larval development and postmetamorphic growth

	# Bundles			Length (μm)			Area (x 10^3 μm^2)		
	Caudal	Rostral	Total	Caudal	Rostral	Total	Caudal	Rostral	Total
Stage 52	73	27	100	170	50	220	4.3	1.0	5.3
Stage 60	244	92	336	340	110	450	11.0	3.7	14.7
Juvenile	242	115	357	370	100	470	14.2	7.7	21.9
Adolescent	254	101	354	390	160	550	16.6	6.3	22.9
Adult	324	113	437	430	180	610	17.5	8.3	25.8

Values in the table were determined from the papillae in Fig. 2. Bundle numbers were determined by counting clearly identifiable stereociliary bundles at high magnification. The SEM images are from curved surfaces that are photographed at slightly oblique angles, hence the length and area measurements are approximate values.

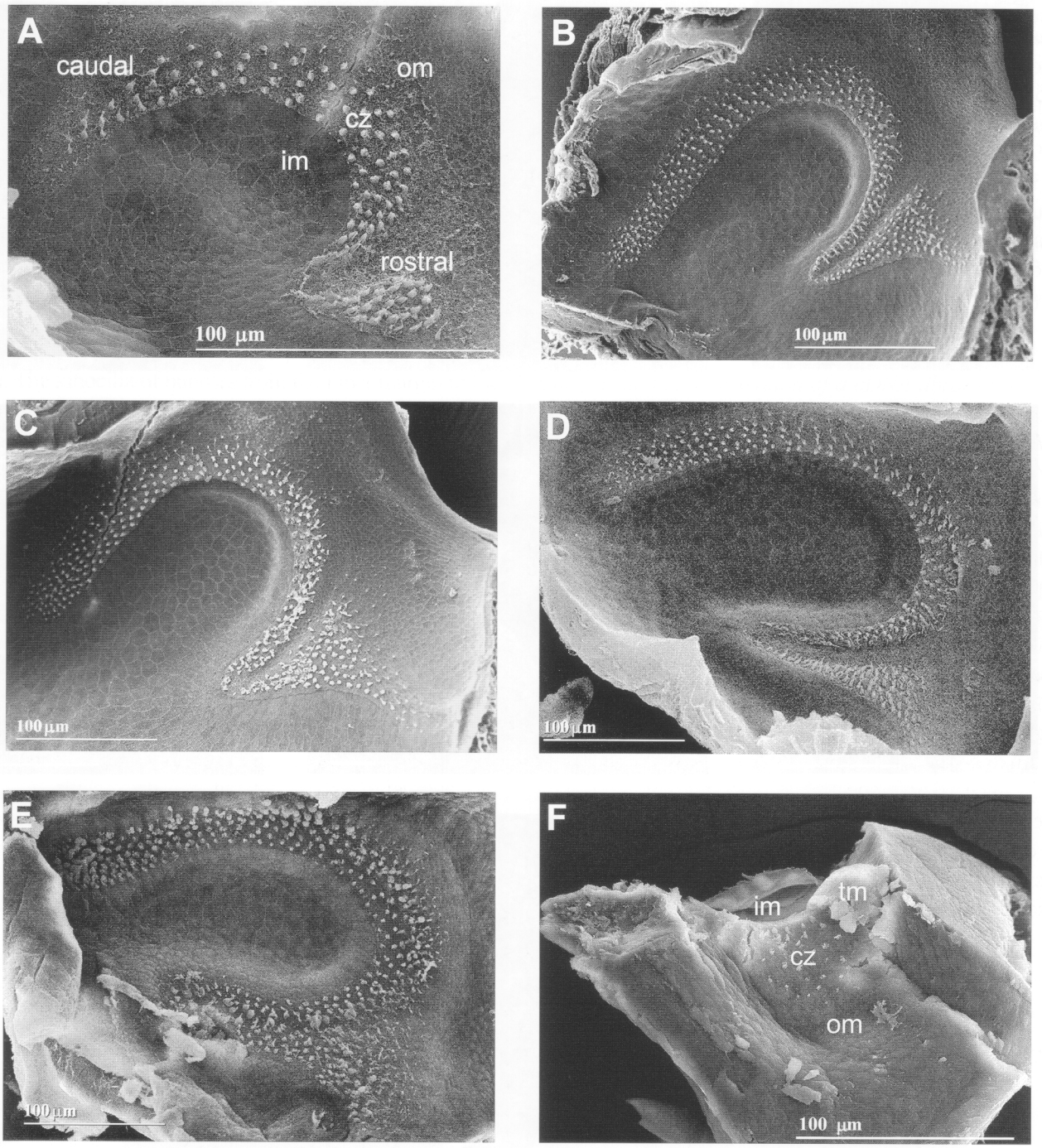

Fig. 2 SEM of the amphibian papilla (**A-E**) and basilar papilla (**F**). Hair cell bundles appear as bright punctate spots on the sensory epithelia. **A**) Stage 52 AP. **B**) Stage 60 AP. **C**) Juvenile AP **D**) Adolescent AP. **E**) Adult AP **F**) Juvenile BP. om: outer margin; cz: central zone; im: inner margin; tm: tectorial membrane. Scale bar 100 μm

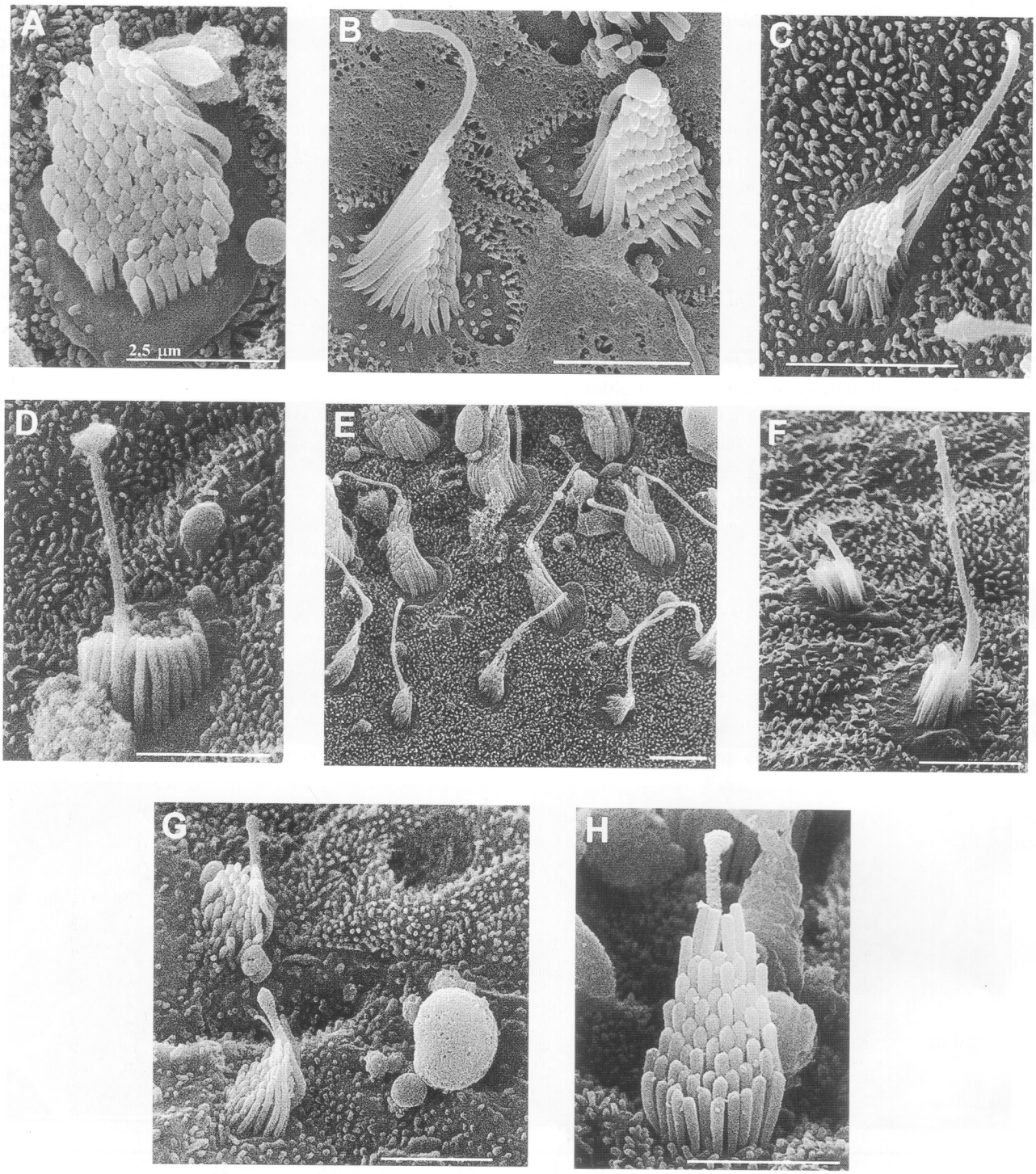

Fig. 3 SEM of hair cell bundles from the amphibian papilla (**A-F**) and basilar papilla (**G**, **H**) of juvenile *Xenopus laevis*. **A)**: AP bundle, inner margin of caudal patch. **B**) AP bundle, central zone of caudal patch. **C**) AP bundle, outer margin of caudal patch. **D**) AP bundle, outer margin of caudal patch. **E**) AP bundles, outer margin of caudal patch. **F**) AP bundles, outer margin of rostral patch. **G**) BP bundle, outer margin. **H**) BP bundle, central zone. Scale bars 2.5 µm

bundles (Fig. 2, Table 1).

A gradation of bundle types is apparent when scanning across the width of the sensory patch from the outer margin (om) through the central zone (cz) to the inner margin (im) along the length of the caudal patch (Fig. 3A-3C). A similar gradation is seen in the rostral patch when scanning from the marginal zone to the cz region. Stereocilia in AP bundles range in height from 1.5 to 5.0 μm, with shorter stereociliary bundles prevalent on the outer margins of the caudal patch (Fig. 3C-3E) and the rostral patch (Fig. 3F). Kinocilia in AP bundles in the outer margins of the caudal patch (Fig. 3C-3E) and the rostral patch (Fig. 3F) can be bulbed or unbulbed. Long kinocilia are usually at least twice the height of the stereocilia and can be either bulbed (Fig. 3A-3D) or unbulbed (Fig. 3E, 3F). The kinocilia of bundles from the inner margin to the central zone of the caudal patch are typically bulbed (Fig. 3A, 3B). In the caudal patch, the number of stereocilia per bundle decreases when scanning across the central zone from the inner to outer margin (Fig. 3A-3C). In the caudal inner margin, bundles can be found that contain over 100 stereocilia (Fig. 3A).

SEM of the basilar papilla

For SEM, the BP was cut in half and the overlying tectorial curtain was removed to expose the bundles. The sensory patch of all ages resembles that of the juvenile specimen (Fig. 2F). As in the AP, bundles are farther apart in the younger than in adult specimens (data not shown). The juvenile BP has between 30-50 bundles, while adult specimens typically have between 40 and 60 bundles.

As in the AP, a gradation of bundle types that crosses the width of the sensory patch from the outer margin (om) through the central zone (cz) to the inner margin (im) can be observed in juvenile and adult specimens. Stereocilia in BP bundles are typically 2.0-4.0 μm in height (Fig. 3G, 3H). Kinocilia in BP bundles are typically bulbed (Fig. 3G, 3H) and it is rare to find an unbulbed kinocilium. There is a tendency for stereocilia to increase in height and for kinocilia to shorten across the outer margin (Fig. 3G) to the central zone (Fig. 3H) and inner margin. As many as 60 stereocilia can be found in a BP bundle (Fig. 3H).

Construction and evaluation of a cDNA library from the inner ear of juvenile X. laevis

The first strand RT synthesis reaction (10 μl) was optimized using cDNA from an initial 2 μg of total RNA template. The second strand cDNA yields obtained from long distance PCR amplification of 2 μl of the first strand reaction ranged from 12 and 20 μg. When aliquots of the second strand cDNA reaction were evaluated by gel electrophoresis prior to size fractionation, cDNA products larger than 10 kb could be detected on the gel (Fig. 4A). The control reaction yielded the expected cDNA products (Clontech), including characteristic bright bands within the cDNA smear that correspond to abundant messages

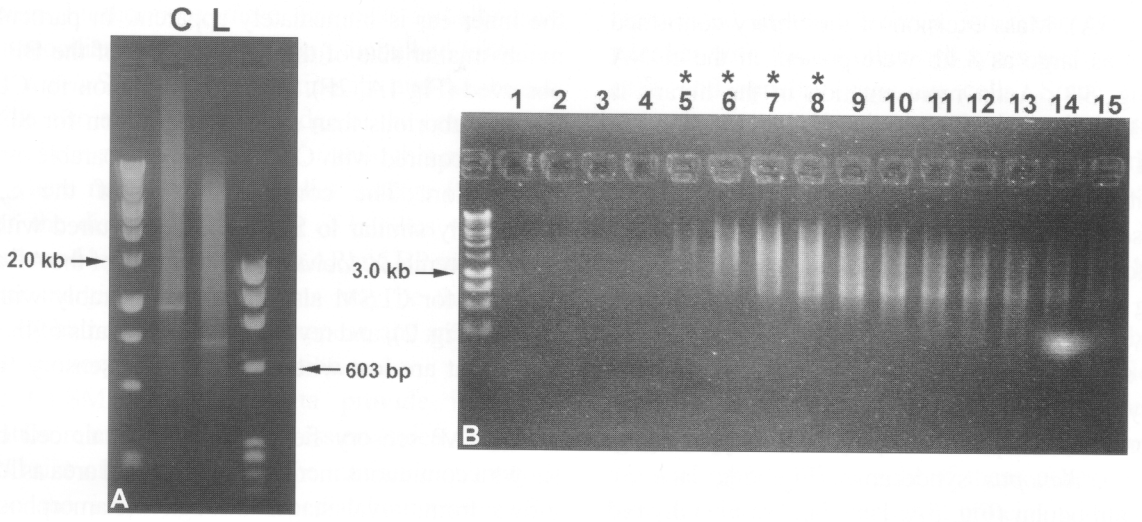

Fig. 4 Synthesis (**A**) and size selection (**B**) of cDNA for cloning. **A**) Gel electrophoresis of of second strand synthesis products from *X. laevis* (L) and control (C) reactions. cDNA as large as 10 kb could be detected on the gel. **B**) Gel electrophoresis of cDNA fractions from column separation. Fractions 5-8 (*) were combined for ligation and packaging.

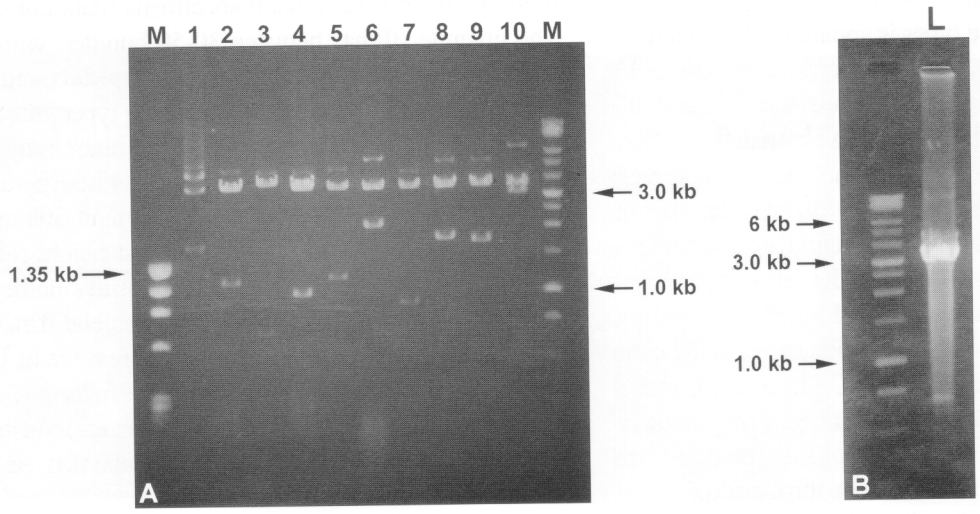

Fig. 5 Evaluation of inner ear cDNA library quality. **A**) Restriction digests of randomly selected clones. **B**: Gel electrophoresis of mass excision of entire *Xenopus* inner ear cDNA library.

(Fig 4A, lane C). Several fractions containing *X. laevis* cDNA and enriched for inserts larger than 800 bp were collected and pooled (Fig. 4B). A portion of the size-fractionated cDNA was ligated to the vector and packaged to construct the primary library. A secondary library with a complexity of 1.5 x 10^6 clones was amplified from the primary library.

The amplified library had a titer of 1.2 x 10^9 pfu/ml, and an average insert size of 1.3 ± 0.7 kb (n= 50) as determined from restriction digests of randomly selected clones (Fig 5A). Mass excision of the library confirmed that inserts as large as 8 kb were present in the cDNA library (Fig. 5B). Actin representation in the library is about 0.3%, increasing the probability that genes expressed in low abundance will be represented (17). Clones with insert sizes greater than 1 kb (1.6 ± 0.7 kb; n= 22) were selected for sequence analysis. Of the 22 clones, 7 coded for sequences for unidentified genes, while the remaining 70% shared between 80%-99% nucleotide identity with sequences posted on GenBank. Based on sequence similarity, examples of clones recovered from the library include: *Xenopus* SNARE protein, *Xenopus* SPARC protein, *Xenopus* RNA polymerase Type 1 (Fig. 5A, lane 1), *Xenopus* syndecan-2 (Fig. 5A, lane 3), *Xenopus* calmodulin (Fig. 5A, lane 5), *Xenopus* thyroid hormone binding protein (pyruvate/kinase), Coenzyme A dehydrogenase, myosin alkali light chain (Fig. 5A, lane 7), and keratin. About 80% of recovered clones were full length sequences containing start sites.

DISCUSSION

Confocal images from the juvenile *X. laevis* inner ear provide an immediate visual appreciation of the complexity of the structure of the auditory apparatus of the inner ear (Fig. 1). The images also illustrate the unique distribution patterns formed by stereociliary bundles in the three auditory organs (Fig. 1). Furthermore, the difference in the number of hair cells between the organs and the relatively small number of auditory hair cells present in the inner ear is immediately apparent. In particular, the much smaller size of the sensory field of the BP can be observed (Fig 1A, 2F). Sample preparation for CLSM is far less laborious than sample preparation for SEM, yet images acquired with CLSM yield comparable structural information. The confocal image of the SAC is remarkably similar to SEM images acquired with SEM from a juvenile *X. laevis* (9). Specimens of the AP and BP prepared for CLSM also compare favorably with SEM images (Fig. 2), and reveal additional details of the whole organ that are lost when exposing the sensory field for SEM.

The AP sensory field defined by hair cell bundles shows a continuous increase in length and area as *X. laevis* grows from larval stages through metamorphosis into mature adults (Fig. 2, Table 1). From stage 52 to the adult age, the length of the sensory field increases by 3 fold and the area by 5 fold. However, the most rapid growth occurs in a 3 week period between stage 52 and stage 60, when

the sensory field doubles in length and triples in area. The number of AP hair cell bundles continues to increase throughout *X. laevis* life (Table 2). Appearance of bundles is most pronounced between larval stages 52 and 60, during which time numbers increase about 3 times from an initial value of ~100 in the stage 52 animal. After metamorphosis, there is a slow and gradual trend for an increase in the number of bundles to a value of over 430 in adult animals (Table 1). In a previous study, similar trends were observed in the *X. laevis* SAC sensory field with animal growth. The number of hair cell bundles in the SAC increases from ~1000 in stage 52 animals, to ~2000 in the juvenile animals, to ~2500 in 2 year adult *X. laevis* (9). The data suggest that in *X. laevis*, auditory hair cells continue to differentiate throughout post-metamorphic development. Whether the appearance of new bundles is associated with mitotic or non-mitotic production of hair cells is unkown at present (3).

The overall morphology of hair cell bundles from the AP and BP resembles what has been previously reported for *Rana catesbeiana* in SEM studies (32). In *X. laevis*, the AP contains bundles with more diverse morphology than the SAC (9) or the BP (Fig. 3). In particular, bundles can be identified in the AP with more stereocilia (50-100) than are observed in the sacculus (9). Both bulbed and unbulbed kinocilia are found in the AP (Fig 3). In both the AP and the BP, the longest kinocilia and the shortest stereocilia are found at the outer margins of the sensory patches. Corwin (7) has shown that in the SAC of *Bufo marinus* newly formed hair cells are found primarily in regions at the edge of the central zone of the sensory epithelium. Furthermore, these hair cells initially have short stereociliary bundles and long, unbulbed kinocilia. In the *X. laevis* SAC, the longest kinocilia and the shortest stereocilia also are found at the edge of the central zone, and it has been proposed that in *X. laevis*, this may be the region where new hair cell bundles emerge (9). Taken together, the distribution patterns of bundles with short stereocilia and long kinocilia in the AP and BP suggest that the outer margins of these organs may be the regions where new hair cell bundles first appear, and are potential zones of auditory hair cell production.

The CLSM and SEM data provide important information relevant to gene expression endeavors. First, the small size of the organs and the miniscule quantity of tissue in the inner ear is immediately apparent. For example, both the AP and the BP are less than 500 μm in a juvenile specimen (Fig. 1). In addition, it can be seen that the number of auditory cells that comprise the *X. laevis* inner ear is very small. While the SAC has some auditory function, the AP and the BP are the main auditory organs in amphibians. In particular, substantial evidence argues that the AP, like the cochlea, is tonotopically organized, with perception of lower frequencies prevalent in the rostral patch and a graduated increase to higher frequencies in the caudal region (31,43). Therefore, a single juvenile inner ear will provide about 500 auditory hair cells for molecular or physiological research. In humans, the cochlea performs its formidable task with about 16,000 hair cells, and inner hair cells that are the primary auditory receptors constitute only several 1000 of these (8,22).

In other molecular studies of the inner ear, construction of cDNA libraries has required 100's of inner ears (19). The strategy presented here uses RT-PCR and takes advantage of methods that use a special oligonucleotide (SMART™, Clontech, CA) in the RT step to synthesize single stranded cDNA that contains the 5' end of the mRNA, thereby increasing the proportion of cDNA in the library that contains full length sequences. When combined with long distance PCR, the cDNA library will contain many large, full length inserts. However, it should be noted that although the λTriplEx2™ vector is stable with inserts between 10-20 kb, the excised plasmids are stable only with inserts up to 7-10 kb (Clontech). These technical constraints limit studies of our excised clones to those that are less than 10 kb.

The first strand cDNA for the library was synthesized from 2 μg of total RNA, a quantity that was isolated from 8 juvenile *X. laevis* ears. We estimate that mRNA from several thousand AP and BP mechanosensory hair cells is represented in the *X. laevis* inner ear cDNA library, together with that of other cell types such as supporting cells and sensory ganglion cells. Since SMART™ technology can be implemented with as little as 50 ng of total RNA, it is useful for investigators working with limited amounts of tissue. In addition to cDNA library construction, it can be used to prepare "virtual" Northerns that can be used to confirm gene expression (12) and to prepare cDNA for microarrays (20).

Results from sequence analysis of randomly selected clones confirmed that most of the identified genes contained the start site of the protein and coded for full length sequences. For some of the identified clones, there are few reports of the role of these genes in inner ear function. The clones represent proteins with a variety of functions. One of the clones coded for SPARC, an extracellular matrix glycoprotein that interacts with growth factors and inhibits cell proliferation (6). Syndecan-2 (46), a membrane proteoglycan that interacts

with both the extracellular matrix and the actin cytoskeleton (47), was also identified by random selection from the inner ear cDNA library. Syndecan-1 has been detected in mouse cochlea (49). Sequence analysis demonstrated that we have cloned calmodulin, a calcium binding protein with a role in mechanoelectrical transduction by hair cells (48), as well as SNARE, a protein that functions in membrane fusion (24). The unconventional myosins, a group of motor proteins, have been implicated in hearing loss (14), thus we noted with interest that one of our clones had sequence homology with myosin alkali light chain (52). Results underscore how cDNA library construction and screening can identify genes and stimulate experimentation aimed at uncovering the role of these proteins in inner ear structure and function. Initially, clones will be used for *in situ* hybridization studies to determine the cellular expression profile of the genes in inner ear organs.

Identification of genes in the inner ear must be followed by experiments aimed at determining gene function, especially of unidentified genes (8). Recently, attention has been drawn to *Xenopus tropicalis* as a viable amphibian model for molecular genetics. This close relative of *X. laevis* offers both the additional advantage of a shorter generation time (3-4 months) and a smaller, diploid genome (2). *X. tropicalis* therefore is potentially a useful organism that may be amenable for genetic studies of the inner ear such as those presented here. In particular, recent technical advances permit transgenic *Xenopus* to be more easily produced, thereby facilitating future tests of the function of unknown genes cloned by our methods (1). Taken together, results presented here suggest that the *Xenopus* inner ear is a useful model for studies of gene expression and auditory system structure and function.

Acknowledgments – We extend our deep appreciation and thanks to Mr. Vincent Lopez-Anaya and Dr. Soumitra Ghoshroy for technical assistance with scanning electron microscopy and helpful discussion during the course of this research. Supported by grants to EES from NIH (NIGMS/NICHD SO6 GM 08136-26; NIDCD DC03292). QAQ is a NIGMS-MBRS RISE graduate trainee and the recipient of a NASA New Mexico space grant consortium fellowship.

REFERENCES

1. Amaya, E. and Kroll, K.L., A method for generating transgenic frog embryos. *Meth. Mol. Biol.* 1999, **97**: 393-414.
2. Amaya, E., Offield, M.F. and Grainger, R.M., Frog genetics: *Xenopus tropicalis* jumps into the future. *Trends Genet.* 1998, **7**: 253-255.
3. Baird, R.A., Steyger, P.S. and Schuff, N.R., Mitotic and nonmitotic hair cell regeneration in the bullfrog vestibular otolith organs. *Ann. N.Y. Acad. Sci.* 1996, **781**: 59-70.
4. Boatright-Horowitz, S.S. and Simmons, A.M., Transient "deafness" accompanies auditory development during metamorphosis from tadpole to frog. *Proc. Natl. Acad. Sci. USA* 1997, **94**: 14877-14882.
5. Bever, M.M. and Fekete, D.M., Ventromedial focus of cell death is absent during development of *Xenopus* and zebrafish inner ears. *J. Neurocytol.* 1999, **28**: 781-793.
6. Brekken, R.A. and Sage, E.H., SPARC, a matricellular protein: at the crossroads of cell-matrix. *Matrix Biol.* 2000, **19**: 569-580.
7. Corwin, J.T., Perpetual production of hair cells and maturational changes in hair cell ultrastructure accompany postembryonic growth in an amphibian ear. *Proc. Natl. Acad. Sci. USA* 1985, **82**: 3911-3915.
8. Corwin, J.T., Identifying the genes of hearing, deafness, and dysequilibrium. *Proc. Natl. Acad. Sci. USA* 1998, **95**: 12080-12082.
9. Díaz, M.E., Varela-Ramírez, A. and Serrano, E.E., Quantity, bundle types and distribution of hair cells in the sacculus of *Xenopus laevis* during development. *Hear. Res.* 1995, **91**: 33-42.
10. Duellman, W.E. and Trueb, L., *Biology of Amphibians*. The Johns Hopkins University Press, Baltimore, 1986, pp. 387-390.
11. Elepfandt, A., Underwater acoustics and hearing in the clawed frog, *Xenopus*. In: *The Biology of Xenopus*, Tinsley, R.C. and Kobel, H.R. (eds.), Clarendon Press, Oxford, 1996, pp. 177-193.
12. Endege, W.O., Steinmann, K.E., Boardman, L.A., Thibodeau, S.N. and Schlegel, R., Representative cDNA libraries and their utility in gene expression profiling. *BioTechniques* 1999, **3**: 542-550.
13. Fettiplace, R. and Fuchs, P.A., Mechanisms of hair cell tuning. *Annu. Rev. Physiol.* 1999, **61**: 809-834.
14. Friedman, T.B., Sellers, J.R. and Avraham, K.B., Unconventional myosins and the genetics of hearing loss. *Am. J. Med. Genet.* 1999, **89**: 147-157.
15. Gallagher, B.C., Henry, J.J. and Grainger, R.M., Inductive processes leading to inner ear formation during *Xenopus* development. *Dev. Biol.* 1996, **175**: 95-107.
16. Haddon, C.M. and Lewis J.H., Hyaluronan as a propellant for epithelial movement: the development of semicircular canals in the inner ear of *Xenopus*. *Development* 1991, **2**: 541-550.
17. Hagen, F.S., Gray, C.L. and Kuijper, J.L., Assaying the quality of cDNA libraries. *BioTechniques* 1988, **6**: 340-345.
18. Hasson, T., Gillespie, P.G., Garcia, J.A., MacDonald, R.B., Zhao, Y., Yee, A.G., Mooseker, M.S. and Corey, D.P., Unconventional myosins in inner-ear sensory epithelia. *J. Cell Biol.* 1997, **137**: 1287-1307.
19. Heller, S., Sheane, C.A., Javed, Z. and Hudspeth, A.J., Molecular markers for cell types of the inner ear and candidate genes for hearing disorders. *Proc. Natl. Acad. Sci. USA* 1998, **95**: 11400-11405.
20. Herrler, M., Use of SMART-generated cDNA for differential gene expression studies. *J. Mol. Med.* 2000, **78**: B23.
21. Holme, R.H. and Steele, K.P, Genes involved in deafness. *Curr. Opin. Genet. Dev.* 1999, **9**: 309-314.
22. Hudspeth, A.J., How hearing happens. *Neuron* 1997, **19**: 947-950.
23. Hudspeth, A.J., Mechanical amplification of stimuli by hair cells. *Curr. Opin. Neurobiol.* 1997, **7**: 480-486.
24. Jahn, R. and Sudhof, T.C., Membrane fusion and exocytosis. *Annu. Rev. Biochem.* 1999, **68**: 863-911.
25. Kay, B.K. and Peng, H.B., *Xenopus laevis*: *Practical Uses in Cell and Molecular Biology*, Acad. Press, Santa Barbara, 1991, pp. 213-230.
26. Kittrell, A.P. and Arjmand, E.M., The age of diagnosis of sensorineural hearing impairment in children. *Int. J. Pediatr. Otorhinolaryngol.* 1997, **40**: 97-106.
27. Kussel-Andermann, P., El-Amraoui, A., Safieddine, S., Nouaille, S., Perfettini, I., Lecuit, M., Cossart, P., Wolfrum, U. and Petit, C.,

Vezatin, a novel transmembrane protein, bridges myosin VIIA to the cadherin-catenins complex. *EMBO J.* 2000, **19**: 6020-6029.
28. Lee, D.J., Gomez-Marin, O. and Lee, H.M., Prevalence of childhood hearing loss. The Hispanic health and nutrition examination survey and the national health and nutrition examination survey. II. *Am. J. Epidemiol.* 1996, **144**: 442-449.
29. Lefebvre, P.P., Van De Water, T.R., Connexins, hearing and deafness: clinical aspects of mutations in the connexin 26 gene. *Brain Res. Rev.* 2000, **32**: 159-162.
30. Lewis, E.R., Baird, R.A., Leverenz, E L. and Koyama, H., Inner ear: Dye injection reveals peripheral origins of specific sensitivities. *Science* 1982, **215**: 1641-1643.
31. Lewis, E.R., Leverenz, E.L. and Koyama, H., The tonotopic organization of the bullfrog amphibian papilla, an auditory organ lacking a basilar membrane. *J. Comp. Physiol.* 1982, **145**: 437-445.
32. Lewis, E.R. and Li, C.W., Hair cell types and distribution in the otolithic and auditory organs of the bullfrog. *Brain Res.* 1975, **83**: 35-50.
33. Lopez-Anaya, V.L., Lopez-Maldonado, D. and Serrano, E.E., Development of the *Xenopus laevis* eighth cranial nerve: Increase in number and area of axons of the saccular and papillar branches. *J. Morphol.* 1997, **234**: 263-276.
34. Martini, A., Mazzoli, M. and Kimberling, W., An introduction to the genetics of normal and defective hearing. *Annu. N.Y. Acad. Sci.* 1997, **830**: 361-374.
35. Mburu, P., Liu, X.Z., Walsh, J., Saw, D. Jr., Cope, M.J., Gibson, F., Kendrick-Jones, J., Steel, K.P. and Brown, S.D., Mutation analysis of the mouse myosin VIIA deafness gene. *Genes Funct.* 1997, **1**: 191-203.
36. McGuirt, W.T. and Smith, R.J., Connexin 26 as a cause of hereditary hearing loss. *Am. J. Audiol.* 1999, **8**: 93-100.
37. Morton, N.E., Genetic epidemiology of hearing impairment. *Ann. N.Y. Acad. Sci.* 1991, **630**: 16-31.
38. Nieukoop, P.D. and Faber, J., *Normal Table of Xenopus laevis* (*Daudin*). North-Holland Publ., Amsterdam, 2nd ed., 1967, pp. I-X.
39. Petit, C., Genes responsible for human hereditary deafness: symphony of a thousand. *Nat. Genet.* 1996, **14**: 385-391.
40. Shofner, W.P. and Feng, A.S., Quantitative light and scanning electron microscopic study of the developing auditory organs in the bullfrog: implications on their functional characteristics. *J. Comp. Neurol.* 1984, **224**: 141-154.
41. Simmons, D.D., Bertolotto, C. and Narins, P.M., Morphological gradients in sensory hair cells of the amphibian papilla of the frog *Rana pipiens pipiens*. *Hear. Res.* 1994, **80**: 71-78.
42. Skvorak Giersch, A.B. and Morton, C.C., Genetic causes of non-syndromic hearing loss. *Curr. Opin. Pediatr.* 1999, **11**: 551-557.
43. Smotherman, M.S. and Narins, P.M., The electrical properties of auditory hair cells in the frog amphibian papilla. *J. Neurosci.* 1999, **19**: 5275-5292.
44. Smotherman, M.S. and Narins, P.M., Hair cells, hearing and hopping: a field guide to hair cell physiology in the frog. *J. Exp. Biol.* 2000, **15**: 2237-2246.
45. Stone, J.S., Oesterle, E.C. and Rubel, E.W., Recent insights into regeneration of auditory and vestibular hair cells. *Curr. Opin. Neurol.* 1998, **11**: 17-24.
46. Teel, A.L. and Yost, H.J., Embryonic expression patterns of *Xenopus* syndecans. *Mech. Dev.* 1996, **59**: 115-127.
47. Trautman, M.S., Kimelman, J. and Bernfield, M., Developmental expression of syndecan, an integral membrane proteoglycan, correlates with cell differentiation. *Development* 1991, **111**: 213-220.
48. Walker, R.G. and Hudspeth, A.J., Calmodulin controls adaptation of mechanoelectrical transduction by hair cells of the bullfrog's sacculus. *Proc. Natl. Acad. Sci. USA* 1996, **93**: 2203-2207.
49. Whitlon, D.S., Zhang, X., Pecelunas, K. and Greiner, M.A., A temporospatial map of adhesive molecules in the organ of Corti of the mouse cochlea. *J. Neurocytol.* 1999, **28**: 955-968.
50. Xiang, C., Wang, H., Sheil, P., Berger, P. and Guerra, D.J., A modified alkaline lysis miniprep protocol using a single microcentrifuge tube. *BioTechniques* 1994, **17**: 30-32.
51. Zakon, H.H. and Wilczynski, W., The physiology of the anuran eighth nerve. In: *The Evolution of the Amphibian Auditory System,* Fritzsch, B., Ryan, M.J., Wilczynski, W., Hetherington, T.E. and Walkowiak, W. (eds.), Wiley and Sons, New York, 1988, pp. 159-184.
52. Zimmermann, K. and Starzinski-Powitz, A., A novel isoform of myosin alkali light chain isolated from human muscle cells. *Nucl. Acids Res.* 1989, **17**: 10496.